Oil Shale, 2024, Vol. 41, No. 4, pp. 237–256
doi: https://doi.org/10.3176/oil.2024.4.01
ISSN 0208-189X

Geochemical characteristics and hydrocarbon potential of source rocks of the Upper Permian Linxi Formation in the Kundu-Taohaiyingzi area, NE China

Yihang Li[(a)], Yujin Zhang[(b)], Xiuli Fu[(c,d)], Renxing Lou[(a)]*, Qingshui Dong[(a,e)], Xiaochao Xin[(a)], Youyou Huang[(a)], Yangxin Su[(c,d)], Yue Bai[(c,d)]

[(a)] College of Earth Sciences, Jilin University, Jilin 130061, China

[(b)] Shenyang Center of Geological Survey, China Geological Survey, Shenyang 110034, China

[(c)] Daqing Oilfield Company Ltd., Exploration and Development Research Institute, Daqing 163712, China

[(d)] National Key Laboratory for Multi-Resources Collaborative Green Production of Continental Shale Oil, Daqing 163000, China

[(e)] Key Laboratory of Oil Shale and Coexisting Minerals of Jilin Province, Changchun 130061, China

Received 23 May 2024, accepted 18 October 2024, available online 31 October 2024

Abstract. *The extremely thick dark mudstone of the Permian Linxi Formation in the Kundu-Taohaiyingzi area of northeastern China is a promising potential area for shale gas prospecting in the periphery of the Songliao Basin. This study involved a geological field survey, outcrop sample collection, and comprehensive geochemical analysis to conduct an in-depth analysis of the organic matter enrichment and hydrocarbon generation potential of the dark mudstone of the target zone, using organic petrology and organic geochemistry. The results show that the thermal maturity of the dark mudstone of the Linxi Formation is in the mature to high-mature stage. The organic matter is dominated by type II kerogen and supplemented by type III kerogen, and the average total organic carbon content is 0.76%, classifying it as a medium-good source rock. The main peak of carbon numbers is primarily distributed between* nC_{17} *and* nC_{19}*, with a smaller amount at* nC_{21}*. The distribution of* n*-alkanes follows a pre-peak pattern characterized by medium and low carbon numbers, suggesting that the organic matter originates from aquatic plants, bacteria, and algae. Combined with the fact that the ratios of pristine and phytane (Pr/Ph) are mainly distributed in the range of 0.99–1.33, the sedimentary environment is a weakly reduced to weakly oxidized lacustrine bay. The systematic analysis of the source rocks of the Upper Permian Linxi Formation in the Kundu-Taohaiyingzi area indicates favorable prospects for shale gas exploration. Utilizing a comprehensive superposition method of geological information, this article identified the Yamen Gacha–Saihan Tala area as a potential area for shale gas exploration.*

* Corresponding author, lourenxing@126.com

Keywords: *Songliao Basin, continental shale, Linxi Formation, geochemical characteristics, hydrocarbon potential.*

1. Introduction

As global demand for petroleum resources continues to grow rapidly, oil and gas exploration faces many new challenges [1]. The huge potential of unconventional shale gas has gained significant interest in recent years [2]. The shale gas revolution has transformed the United States into a net exporter of oil and gas. Shale gas, produced from dark mudstone rich in organic matter with extremely low porosity and permeability, mainly exists in mud shale reservoirs either in a free or adsorbed state [3, 4]. These typical characteristics make shale gas reservoirs highly resistant to damage [5], allowing them to form in formations where conventional oil and gas reservoirs are difficult to gather and preserve.

The Kundu-Taohaiyingzi area is located in the eastern part of the Central Asian orogenic belt on the periphery of the western margin of the Songliao Basin, characterized by strong volcanic activity [6, 7]. The stratigraphy of the Linxi Formation is widely distributed, with thick sequences of dark mudstone, which provides a potential material base and storage site for shale gas [8, 9].

A series of studies on the hydrocarbon source rocks of the Kundu-Taohaiyingzi area in northeastern China have been carried out by previous researchers. Studies indicate that the average total organic carbon (TOC) content of the source rocks in the Linxi Formation is 0.58–0.72%, with moderate organic matter abundance. The main type of kerogen is type II, with some occurrences of type III, categorizing these source rocks as medium to good in quality [10, 11]. The thermal maturity of the dark mudstone in the Linxi Formation is relatively high, with organic-matter vitrinite reflectance (R_o) values ranging from 2.0 to 4.5%, placing the rocks in the high-mature to over-mature stage [12, 13]. This suggests that the source rocks in this region predominantly generate gas rather than oil [14].

Previous studies on the Linxi Formation in the Kundu-Taohaiyingzi area have mainly focused on local or conventional organic geochemical testing and analysis, which present certain limitations. Firstly, relying solely on organic carbon content and kerogen type provides an incomplete assessment of the hydrocarbon generation potential of the source rocks. Secondly, the high thermal maturity of the study area makes a single parameter insufficient to accurately evaluate the hydrocarbon generation potential. While current methods, such as gas chromatography–mass spectrometry (GC–MS) and kerogen carbon isotope analysis, offer valuable data, they may present uncertainties when applied to different geological contexts. In view of the high degree of organic matter evolution in this area, a more in-depth systematic analysis using unconventional multi-parameter organic geochemistry would

be important to objectively understand the hydrocarbon generation and accumulation prospects of the dark mudstone under review [15].

Through systematic observation, sampling of field outcrop profiles, and various analytical techniques – including hydrocarbon potential assessment, organic microcomponent analysis, multi-parameter maturity characterization, GC–MS, and kerogen carbon isotope analysis –, this study conducts an in-depth examination of the distribution characteristics and hydrocarbon potential of the dark mudstone of the Linxi Formation, located in the Kundu-Taohaiyingzi area of northeastern China. Additionally, the comprehensive overlay method of geological information was employed to predict the favorable exploration target area for shale gas, with a view to providing a scientific basis for future shale gas exploration in the region.

2. Geological setting

The Kundu-Taohaiyingzi area is situated in the western part of the Songnen Massif, on the southwestern edge of the Songliao Basin in northeastern China (Fig. 1). The Late Permian Linxi Formation was formed during an important transition from the Paleo-Asian Ocean to the Pacific Ocean tectonic domain [16–22]. Under the influence of the compression and collision of the Siberian Plateau and North China Plateau, the study area experienced multiple tectonic events in the Late Paleozoic [23]. During the Late Carboniferous to the Middle Permian, the study area was in a relatively stable extensional tectonic environment and developed a set of large-scale marine sediments. The ancient Asian Ocean was in a closed state from the Late Middle Permian to the Early Triassic. The seawater in the study area retreated during the evolutionary process from the marine phase in the Early Permian to the marine–continental phase in the Late Permian, which eventually led to the formation of a continental environment [24, 25].

The Upper Permian Linxi Formation (P_3l) is the latest continental lake basin deposit in the above tectonic context [26, 27]. The rock assemblage within this formation is primarily composed of yellow-green fine sandstone, gray-black siltstone, gray-black mudstone, and dark gray shale, with stratigraphic thicknesses of 475–2900 m. Regionally, the Linxi Formation is in a conformable contact with the underlying Middle Permian Zheshi Formation and the overlying Triassic Laolongtou Formation. However, the Laolongtou Formation is largely absent and is mostly unconformably covered by Jurassic or Cretaceous strata. The Linxi Formation is characterized by the development of thick lacustrine dark mudstone, with a thickness of 105–975 m. A large amount of sporopollen fossils (*Kraeuselisporites spinulosus*, *Urmites complicates*), plant fossils (*Paracalamites*, *Noeggerathiopsis*), and abundant freshwater lamellibranchian fossils can be seen in the mudstone (Fig. 2) [28, 29].

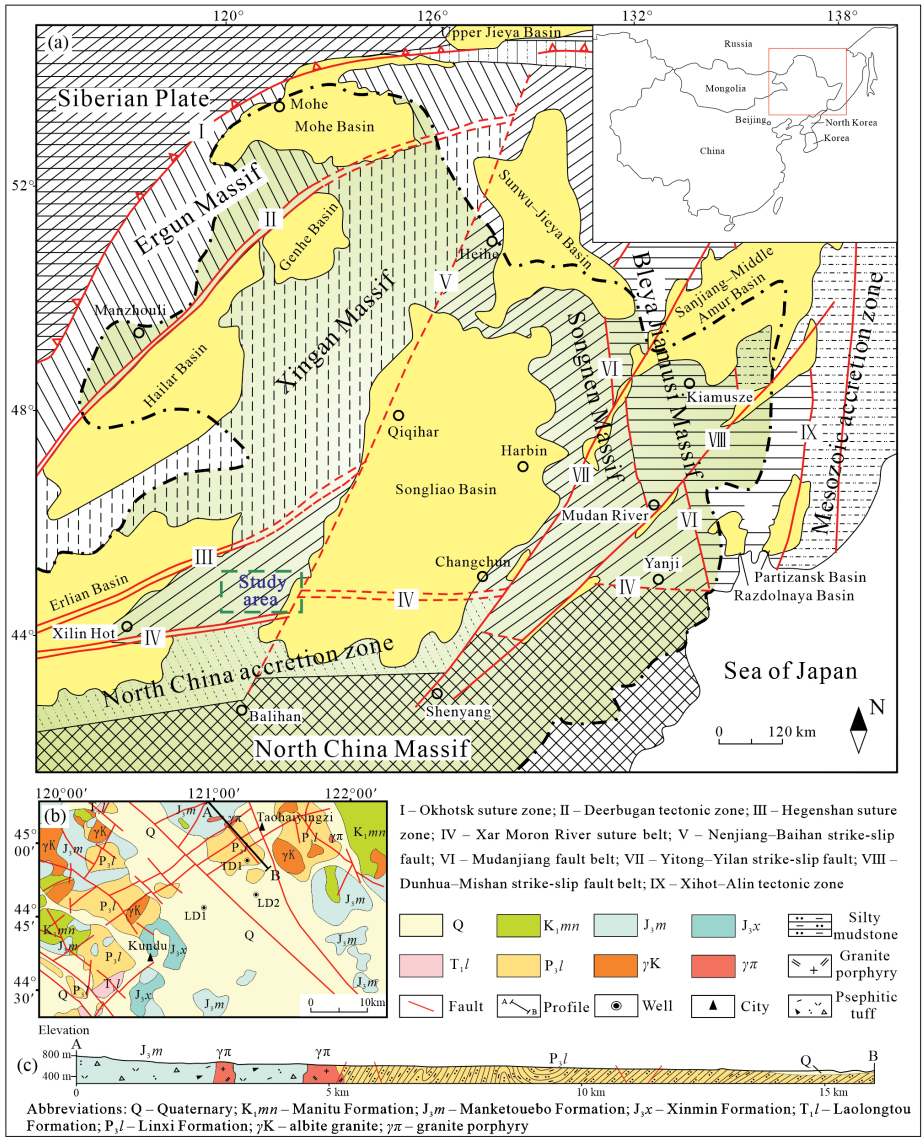

Fig. 1. Regional tectonic background and location map of the Kundu-Taohaiyingzi area in northeastern China, revised from [21] (a), geological map (b), and typical geological profile of the area (c). The color figure is available in the online version of this journal.

3. Samples and methods

Due to limited drilling in the research area, all samples of the Linxi Formation were collected from outcrop sampling, with a total of 23 dark mudstone samples obtained. The testing of samples was primarily conducted at the College of Resources and Environment of Yangtze University. The testing included TOC measurement, rock pyrolysis, kerogen carbon isotope analysis, microcomponent identification, and GC–MS analysis of saturated hydrocarbons.

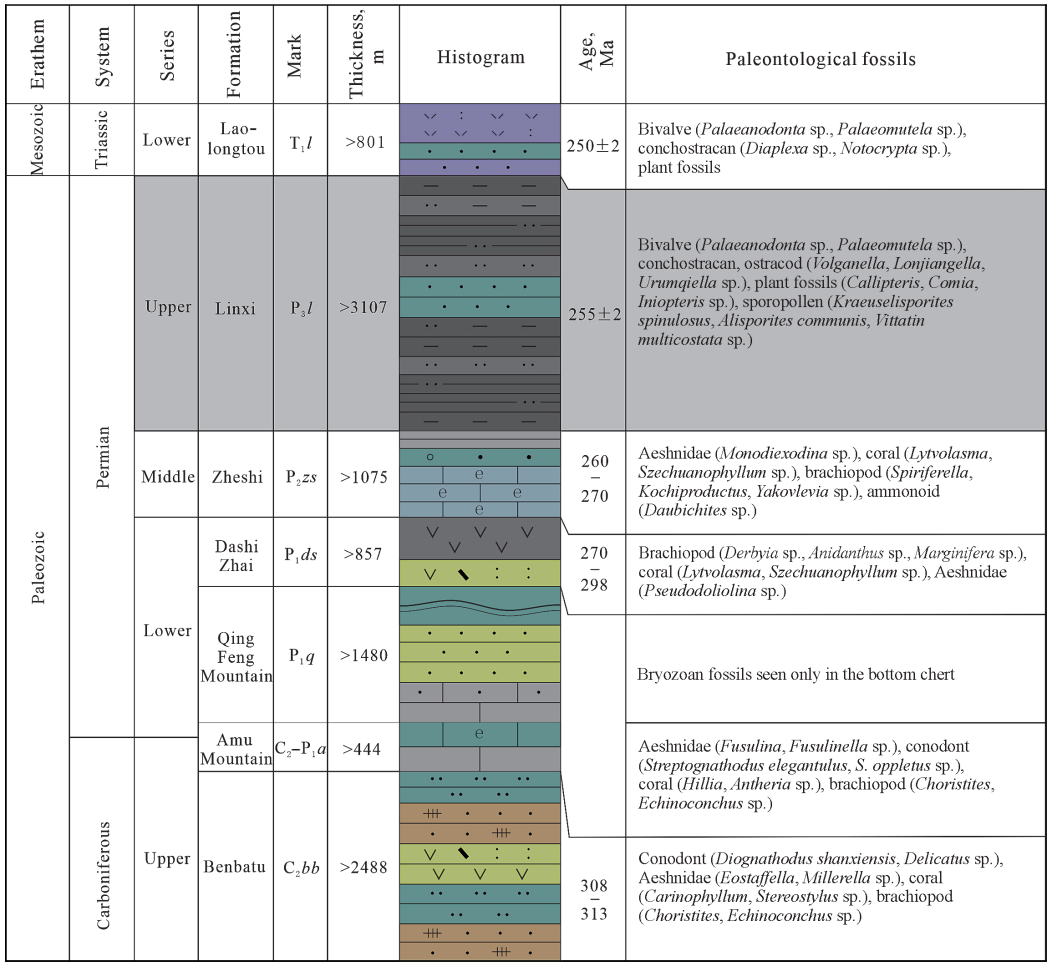

Note: The age data of P_3l and T_1l are from actual measurements, and the rest of age data are quoted from Zheng et al. (2018).

Fig. 2. Comprehensive stratum histogram of the Late Paleozoic in the Kundu-Taohaiyingzi area, revised from [48].

3.1. TOC and rock pyrolysis

The mudstone was crushed to below 0.08 mm and freeze-dried to obtain the samples. Approximately 80–120 mg of the samples were weighed into a crucible, inorganic carbon was removed using dilute hydrochloric acid, and the TOC content was then measured. The samples were automatically analyzed using an OGE-VI instrument. During the pyrolysis analysis, the instrument was rapidly heated to 300 °C and maintained at this temperature for three minutes to measure the content of free hydrocarbons (S_1). Subsequently, the temperature was raised to 600 °C at a rate of 50 °C/min and maintained at this temperature for one minute to determine the content of pyrolyzed hydrocarbons (S_2).

3.2. Separation of quantitative group components and GC–MS analysis of saturated hydrocarbons

The samples were extracted using a Soxhlet extractor for 72 hours to obtain the chloroform asphalt, referred to as "A". After precipitation and filtration of the asphaltene with *n*-hexane, a silica-alumina (2:3) column was used to separate the components. The hydrocarbon ingredients were eluted with *n*-hexane, *n*-hexane-dichloromethane (2:1), and dichloromethane-methanol (97:3). The GC–MS analysis of the saturated hydrocarbons was performed using an Agilent 6890/5975 desktop mass spectrometer and an HP-5 MS quartz elastic capillary column (30 m × 0.25 mm × 0.25 μm). This experiment used helium as the carrier gas and adopted a detection method of full scan with multi-ion detection.

4. Discussion and analysis

4.1. Organic geochemical characteristics

4.1.1. Organic matter maturity

The temperature of maximum hydrocarbon generation (T_{max}), the odd-even predominance index (OEP), and the carbon predominance index (CPI) were used to determine the maturity of organic matter in the dark mudstone of the Linxi Formation. The results indicated that the dark mudstone in this area generally falls within the mature to high-mature stages, where the T_{max} values are mainly distributed between 444–574 °C. Two samples exhibit T_{max} values between 440–450 °C, placing them within the mature stage. In addition, 12 samples display T_{max} values between 450–580 °C, indicating a high-mature stage (Fig. 3).

The OEP and CPI are effective in determining the maturity of samples [30–32]. The CPI test values of the samples from the study area range from 1.10 to 1.15 and the OEP test values from 1.02 to 1.03, both of which are

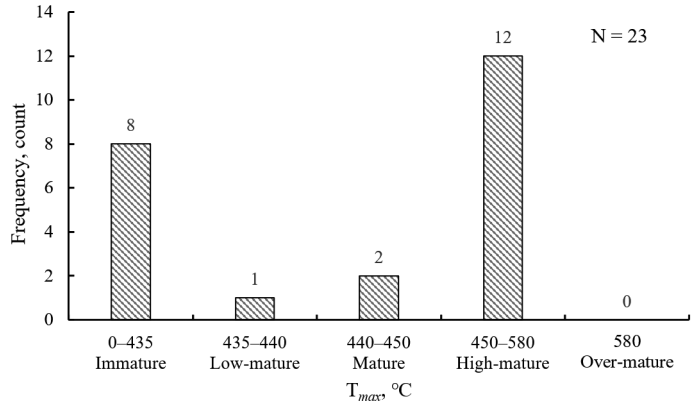

Fig. 3. Distribution histogram of the highest pyrolysis peak temperature (T_{max}) of organic matter in the Linxi Formation in the Kundu-Taohaiyingzi area.

below 1.20 (Table 1). These values clearly indicate mature organic matter, which is consistent with the characteristics shown by the T_{max} of the samples.

Table 1. Saturated hydrocarbon parameters of source rocks in the Kundu-Taohaiyingzi area

Sample	CPI	OEP	Pr/nC_{17}	Ph/nC_{18}	Pr/Ph	$nC_{10–21}/nC_{15–32}$
2017TY03	1.13	1.02	0.18	0.16	0.99	1.00
D1052TY01	1.15	1.02	0.06	0.05	1.13	2.56
D1052TY02	1.10	1.02	0.08	0.06	1.33	1.81
D5469TY02	1.12	1.02	0.16	0.13	1.15	1.75
D5524TY01	1.11	1.03	0.04	0.04	1.09	1.32

Therefore, the comprehensive analysis shows that the organic matter in the Linxi Formation of the Kundu-Taohaiyingzi area has undergone a high degree of thermal evolution, placing it generally in the mature to high-mature stages, with potential for hydrocarbon generation.

4.1.2. Organic matter types

In this study, the organic matter types of the source rocks were comprehensively evaluated using microscopic components and kerogen carbon isotope indexes.

Microscopic identification of the microscopic components of the five samples in the profile revealed that they are mainly composed of amorphous components of the sapropelic group and unstructured vitrinite of the vitrinite

group (Fig. 4), accounting for 48–57% and 31–36%, respectively (Fig. 5). Different kerogen microcomponents contribute variably to hydrocarbon generation, and the organic matter type index (TI) can be used to classify the type of organic matter. The formula is as follows:

$$TI = \frac{A \times 100 + B \times 50 + C \times (-75) + D \times (-100)}{100}, \quad (1)$$

where A, B, C, and D are the percentages of amorphous components, exinite, vitrinite, and inertinite, respectively.

The TI values of the five samples ranged from 27 to 37. Based on the classification standard for kerogen microscopy in China's oil and gas industry (SY/T 5735-1995) [33], the organic matter in the dark mudstone in the Linxi Formation should be mainly sapropel-humic type II_2.

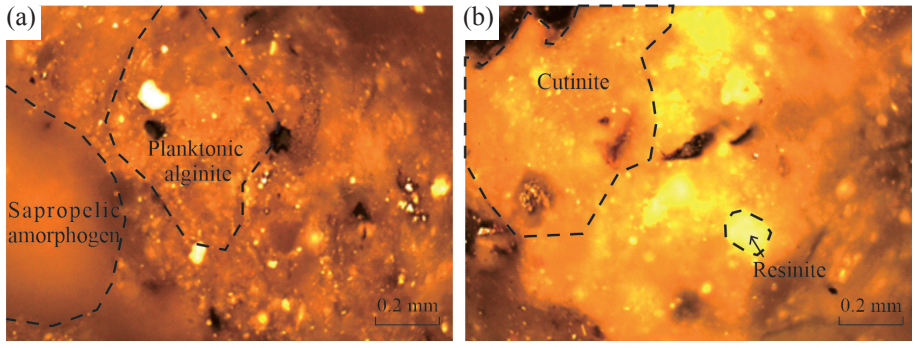

Fig. 4. Microscopic component characteristics of kerogen in the Linxi Formation in the Kundu-Taohaiyingzi area: samples 2017TY03 (a) and D1052TY02 (b).

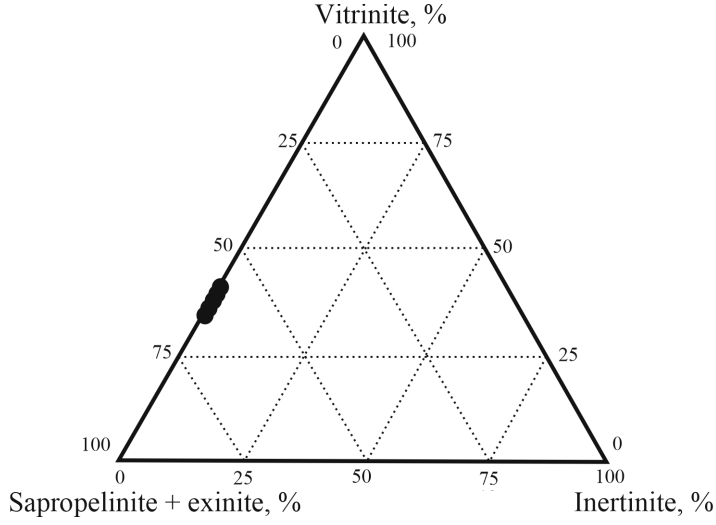

Fig. 5. Triangle diagram of kerogen microscopic components in the dark mudstone of the Linxi Formation.

There are significant differences in isotopic composition among different types of kerogen. Sapropel kerogen is relatively enriched in light carbon isotopes ($\delta^{12}C$) [34, 35], whereas humic kerogen is relatively enriched in heavy carbon isotopes ($\delta^{13}C$) [36]. Therefore, the carbon isotope composition of kerogen is an important indicator for classifying the kerogen types of continental source rocks.

Tests show that the $\delta^{13}C$ values of the five hydrocarbon source rocks of the Upper Permian Linxi Formation are mainly distributed between –28 and –25.5‰. Based on the classification standard for kerogen microscopy in China's oil and gas industry (SY/T 5735-1995), the kerogen should be classified as type II. Considering that $\delta^{13}C$ is significantly influenced by thermal maturity, there is typically a variation of 2 to 6‰ due to thermal alteration [37–39]. Therefore, given the high degree of thermal evolution of the source rocks of the Linxi Formation in the study area, the obtained values of $\delta^{13}C$ were somewhat reweighted. While the organic matter in these source rocks is still predominantly type II kerogen, it may also contain some type III kerogen.

4.1.3. Organic matter abundance

Organic matter abundance is assessed using indicators such as TOC, chloroform pitch "A", and hydrocarbon potential ($S_1 + S_2$) [40]. Since the dark mudstone of the Linxi Formation in the study area is in a mature to high-mature stage of thermal evolution, the peak of hydrocarbon production has already ended. As a result, the residual hydrocarbon generation potential of the kerogen is very low. The chloroform pitch "A", total hydrocarbon content (HC), and hydrocarbon potential ($S_1 + S_2$) in these source rocks have become very low and cannot be compared with known source rocks under low maturity conditions. Therefore, in this study, the stacking evaluation method of residual TOC and $S_1 + S_2$ was used to evaluate the organic matter abundance in the dark mudstone of the Linxi Formation.

Tests show that the TOC values of the source rocks of the Linxi Formation in the study area are distributed between 0.37 and 1.21% (Table 2), with an average value of 0.76%. Among them, 13 samples reached the standard of medium shale gas source rock, while three samples qualified as good shale gas source rock. Further analysis of residual organic carbon content and hydrocarbon potential shows that the source rocks of the Linxi Formation in the study area are generally classified as medium-good hydrocarbon source rocks (Fig. 6).

In comparison, the Barnett Shale, which has been extensively studied, formed in a marine environment, resulting in high organic matter content and good quality. In contrast, the source rocks of the Linxi Formation in the study area are primarily lacustrine in origin, with all samples collected from outcrops. Consequently, the TOC and hydrocarbon potential of the source rocks in the study area are relatively low, with most samples classified as medium-good hydrocarbon source rocks.

Table 2. Comprehensive evaluation data of Linxi Formation source rocks in the Kundu-Taohaiyingzi area

Serial number	Sample number	TOC, %	$S_1 + S_2$, mg/g	T_{max}, °C	$\delta^{13}C$‰, PDB
1	2017TY01	1.13	1.15	289	n/a
2	2017TY02	0.93	0.16	426	n/a
3	2017TY03	0.99	0.49	513	–25.72
4	D1052TY01	0.70	0.06	450	–26.47
5	D1052TY02	0.78	0.02	441	–25.89
6	D5469TY02	0.83	0.05	504	–25.76
7	D5524TY01	0.87	0.19	574	–26.70
8	2017TY04	1.21	0.12	417	n/a
9	D5469TY01	0.86	0.03	439	n/a
10	D3018TY01	0.39	0.08	466	n/a
11	2017TY05	0.57	0.02	350	n/a
12	2017TY06	0.78	0.08	461	n/a
13	2017TY07	0.37	0.49	306	n/a
14	2017TY08	0.59	0.11	348	n/a
15	2017TY09	0.74	0.01	514	n/a
16	2017TY10	0.62	0.01	521	n/a
17	2017TY11	0.60	0.01	531	n/a
18	2017TY12	0.68	0.01	532	n/a
19	PM211TY163	0.60	0.02	444	n/a
20	PM212TY15	0.64	0.04	486	n/a
21	PM212TY42	1.16	0.04	466	n/a
22	PM212TY46	0.58	0.16	370	n/a
23	D8257TY1	0.80	0.02	348	n/a

n/a – not applicable

4.2. Characterization of organic matter genesis and hydrocarbon potential

4.2.1. Origin and characteristics of isoprene alkanes

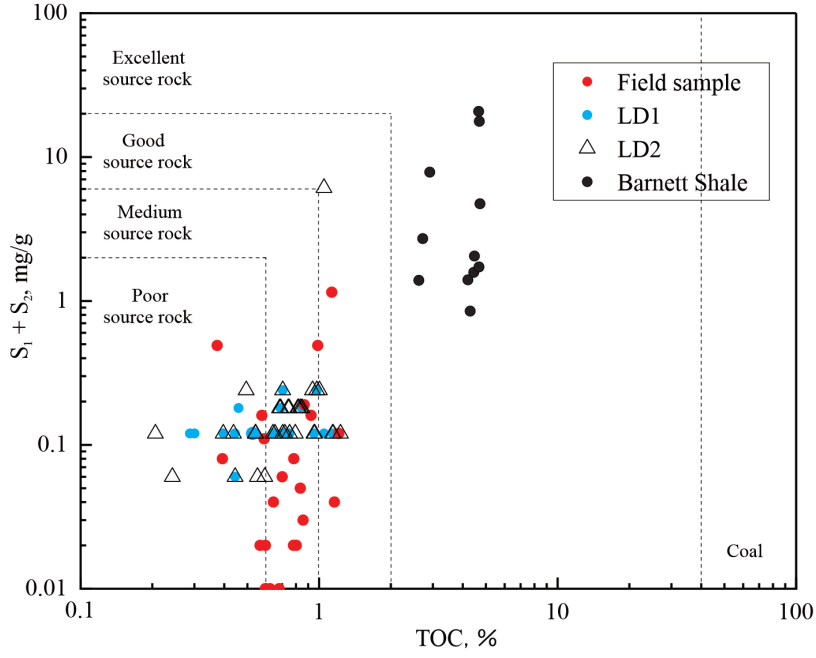

Fig. 6. Cross-plot of organic carbon content and hydrocarbon generation potential of the Linxi Formation source rocks. The data of well LD1, well LD2, and Barnett Shale are cited in [10], [49], and [50].

Isoprene alkanes are a class of biomarkers that can indicate the source of organic matter and sedimentary environments [41]. Among these, pristane (Pr) and phytane (Ph) are the most abundant and widely distributed, originating largely from the chlorophyll a of photosynthetic organisms and the phytol side-chains of bacterial chlorophyll a and b in purple sulfur bacteria. Generally, a Pr/Ph ratio of <0.5 indicates strongly reducing depositional environments, 0.5–1.0 suggests reducing environments, 1.0–2.0 shows weakly reducing to weakly oxidizing environments, and >2.0 is seen in oxidizing environments [42].

The Pr/Ph ratios of outcrop samples from the Linxi Formation mainly range from 0.99 to 1.33, with an average value of 1.14, indicating a weakly reducing to weakly oxidizing depositional environment. In addition, the correlation between Pr/nC$_{17}$ and Ph/nC$_{18}$ can indicate the formation environment of organic matter and its type [43]. Based on the distribution of the intersection points of Pr/nC$_{17}$ and Ph/nC$_{18}$, it is inferred that the study area was formed in a weakly reducing to weakly oxidizing depositional environment. Preliminary assessment suggests that the organic matter type in this area should be type II$_2$ (Fig. 7). This identification coincides with the organic matter type of the region as determined from the organic geochemical indicators described previously.

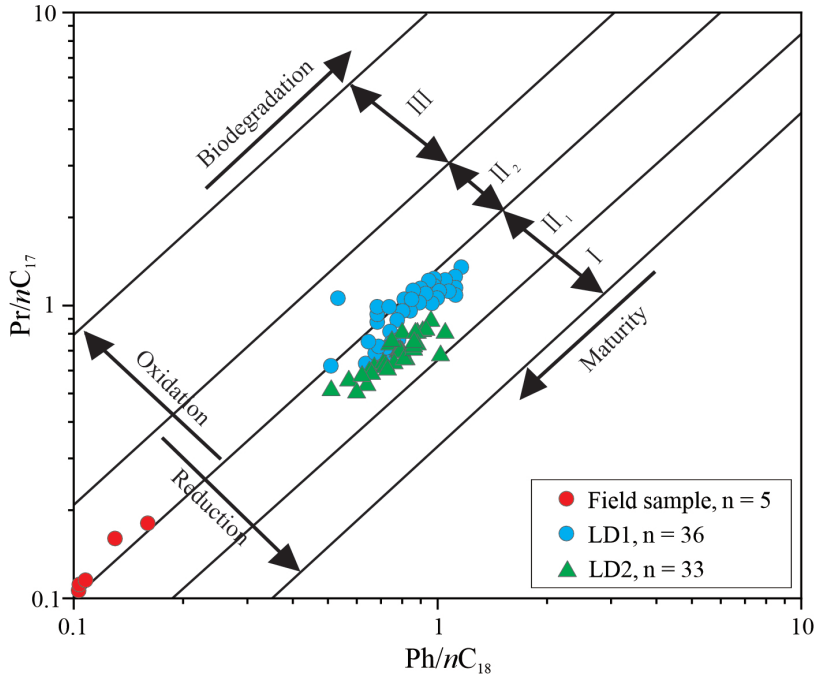

Fig. 7. Cross-plot of Pr/nC$_{17}$ and Ph/nC$_{18}$ of the Linxi Formation source rocks.

4.2.2. Genetic characteristics of *n*-alkanes

Previous research indicates that low-carbon-numbered *n*-alkanes (<nC$_{20}$) are derived from algae and microorganisms, while medium-carbon-numbered *n*-alkanes (nC$_{21}$–nC$_{25}$) are derived from peat moss and emergent aquatic plants [44–47]. Based on the saturated hydrocarbon chromatographic analysis of four outcrop samples in the target zone (Fig. 8), the carbon number distribution of *n*-alkanes in this area ranges from nC$_{15}$ to nC$_{32}$, with the main peak carbon numbers primarily distributed in nC$_{17}$–nC$_{19}$, and a small amount in nC$_{21}$.

Specifically, the *n*-alkane carbon number distribution in sample D1052TY01 from Qiaoluotu Mountain in the southwestern part of the study area, and in samples D5469TY02 and D5524TY01 from Taohaiyingzi in the north-central part, shows a pre-peak pattern of low carbon number. This indicates that the organic matter originates from the algae and microorganisms in the environment of deeper-water lakes and bays. However, the *n*-alkane carbon number distribution in sample 2017TY03 from Habutegai in the west-central part of the study area displays a pre-peak pattern of medium carbon number, suggesting a source from mosses and emergent plants in the edge environment of shallow lake bays. Therefore, it is speculated that the organic matter supply of the Linxi Formation in the study area is from lacustrine sediments in a terrestrial environment.

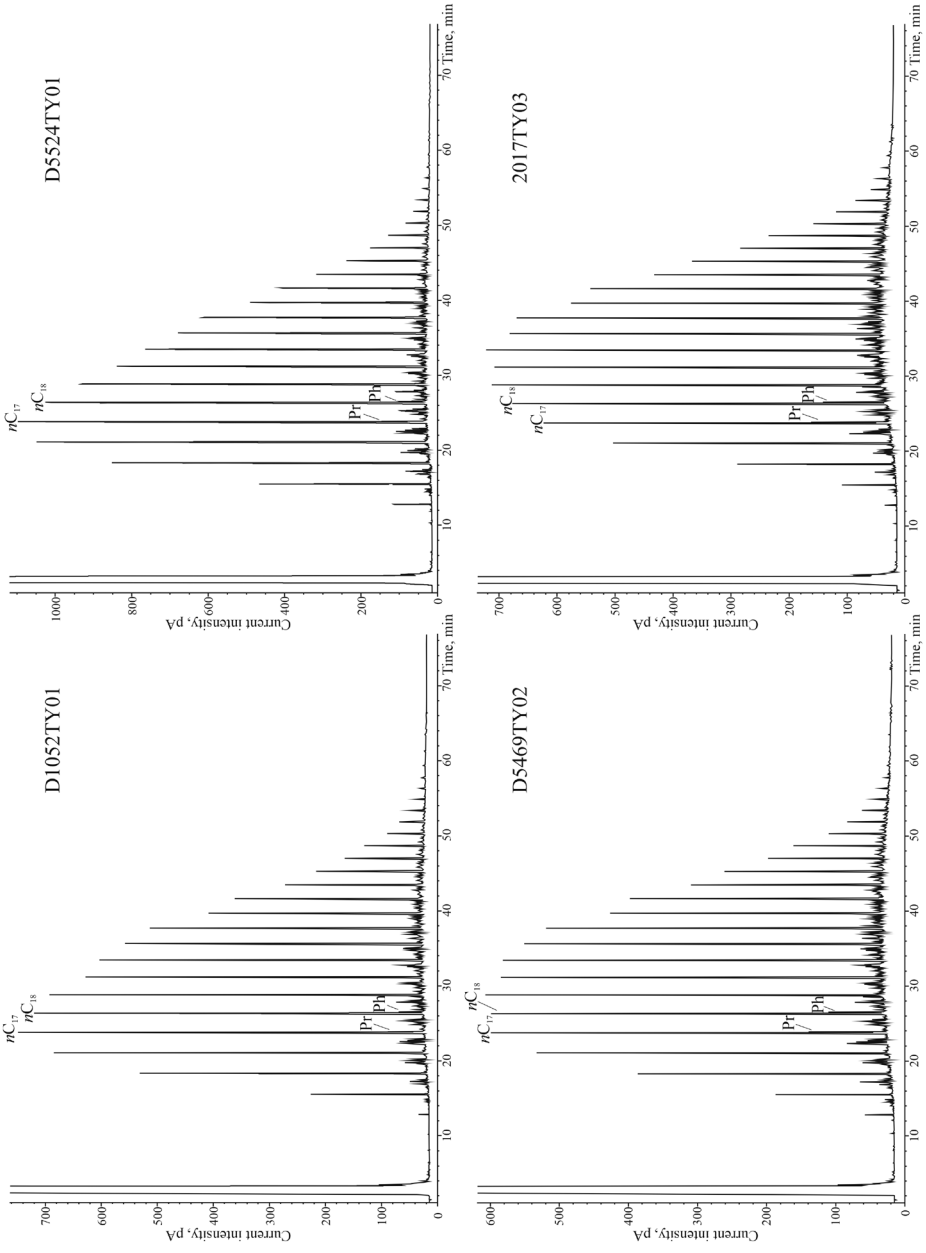

Fig. 8. Gas chromatography peak diagram of saturated hydrocarbons in the Linxi Formation in the Kundu-Taohaiyingzi area.

4.3. Hydrocarbon generation potential and prediction of favorable prospect areas

As can be seen from the above, the Linxi Formation in the Kundu-Taohaiyingzi area has developed medium to good hydrocarbon source rocks, which were formed in a lake bay environment with weak reduction to weak oxidation in a lacustrine environment. Combined with the observations and measurements of outcrop sections in this zone, it can be found that the dark mudstone of the Linxi Formation is widely distributed and exhibits great thickness. It can be inferred that the medium-good source rocks in the Kunlun-Taohaiyingzi area have significant development and resource potential.

Based on the comprehensive study of the distribution characteristics of dark mudstone thickness, organic matter abundance, and maturity parameter T_{max} in the study area, it is preliminarily suggested that the Yamen Gacha–Saihan Tala zone is a favorable prospect area. The pyrolysis peak temperature T_{max} in this area is >435 °C, the organic matter is in the mature to high-mature stage, and the average abundance of organic matter is >0.6%. The thickness of medium-good source rock is >500 m. It is the most favorable prospective region for shale gas exploration in the Kundu-Taohaiyingzi area (Fig. 9), with an exploration area of approximately 336 km^2.

5. Conclusions

1. The T_{max} values of the dark mudstone of the Linxi Formation in the Kundu-Taohaiyingzi area mainly range from 444 to 574 °C, with the CPI and OEP test values below 1.20, reflecting that the organic matter is in the mature to high-mature stage. Kerogen microscopic examination shows TI values between 27 and 37, and $\delta^{13}C$ values are distributed between –28 and –25.5‰, which comprehensively reflects that the kerogen is predominantly type II, with some type III. The TOC content is 0.37–1.21%, averaging 0.76%, classifying it as a medium-good source rock.
2. The carbon number distribution of *n*-alkanes in the Linxi Formation is dominated by low carbon number pre-peak types, supplemented by medium carbon number pre-peak types. The pristine/phytane ratios (Pr/Ph) are between 0.99 and 1.33, with an average value of 1.14. This suggests that the organic matter originates from a mixture of lower aquatic organisms, such as emergent plants, bacteria, and algae. The comprehensive data show that its sedimentary environment was a lake bay facies with weak reduction and weak oxidation.
3. The Yamen Gacha–Saihan Tala zone in the central part of the study area exhibits a peak temperature of thermal decomposition (T_{max}) greater than 435 °C, indicating that the organic matter has reached a mature to high-mature stage of evolution. The average abundance of organic matter is

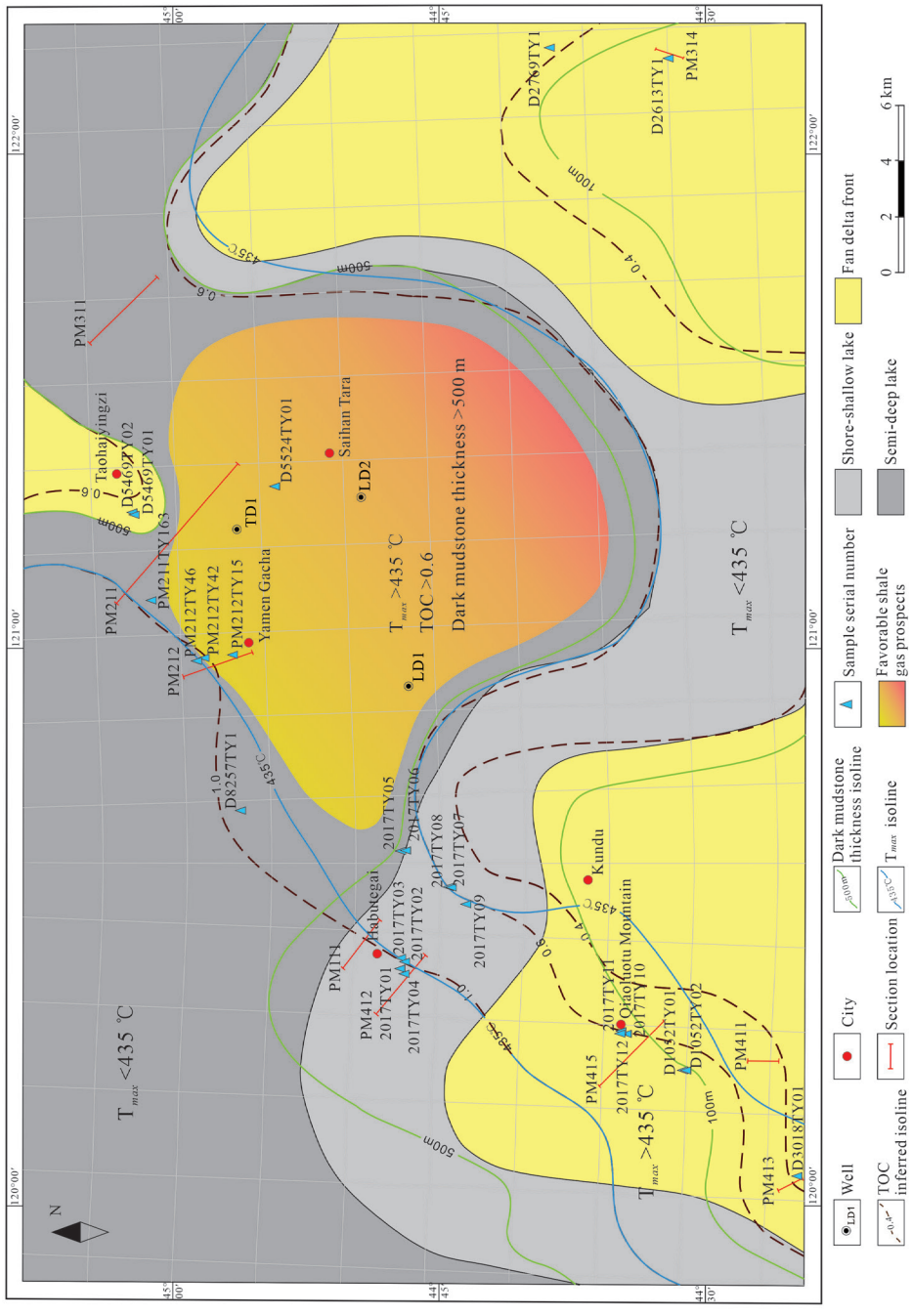

Fig. 9. Forecast map of shale gas potential in the Linxi Formation in the Kundu-Taohaiyingzi area. The color figure is available in the online version of this journal.

greater than 0.6%, and the thickness of the medium-good hydrocarbon source rocks exceeds 500 m. It is currently the most favorable prospective area for shale gas exploration in the Kundu Taohaiyingzi area of northeastern China, with an exploration area of 336 km^2.

Acknowledgments

The work was funded by the National Key Research and Development Program for Young Scientists (grant No. 2021YFC2900200), the China Geological Survey Project (grants No. DD20160048-04 and No. DD20230220), and the China National Petroleum Corporation's (CNPC) Major Science and Technology Project (grant No. 2023ZZ15). The author sincerely thanks all reviewers for their abundant critical and constructive comments. The publication costs of this article were partially covered by the Estonian Academy of Sciences.

References

1. Wu, Z., Peng, S., Du, W. Coal-measure source rock characteristics and burial evolution history in the Shisanjianfang Area, Tuha Basin. *Arabian J. Geosci.*, 2016, **9**(5), 417. https://doi.org/10.1007/s12517-016-2438-2
2. Sun, P., Li, W., Liu, Z., Niu, D., Wu, X., Tao, L., Wang, Z., Luan, Z. Selection of favourable targets for the in-situ conversion of continental oil shale in China. *Oil Shale*, 2023, **40**(3), 177–193. https://doi.org/10.3176/oil.2023.3.01
3. Maravelis, A. G., Chamilaki, E., Pasadakis, N., Vassiliou, A., Zelilidis, A. Organic geochemical characteristics and paleodepositional conditions of an Upper Carboniferous mud-rich succession (Yagon Siltstone): Myall Trough, southeast Australia. *J. Pet. Sci. Eng.*, 2017, **158**, 322–335. https://doi.org/10.1016/j.petrol.2017.08.065
4. Mi, S., Guo, Q., Zhang, Q., Wang, J. Classification and potential of continental shale oil resources in China and resource evaluation methods and criteria. *Oil Shale,* 2023, **40**(4), 283–320. https://doi.org/10.3176/oil.2023.4.02
5. Mou, C. L., Wang, X. P., Wang, Q. Y, Ge, X. Y., Zan, B., Zhou, K. K., Chen, X. W., Liang, E. *Lithofacies Paleogeography and Geological Survey of Shale Gas*. Springer, Singapore, 2023.
6. Lou, R., Dong, Q., Nie, H. Exploration prospects of shale gas resources in the Upper Permian Linxi Formation in the Suolun-Linxi Area, NE China. *Energy Fuels*, 2017, **31**(2), 1100–1107.
7. He, W., Shan, X., Sun, Y., Cao, H., Zheng, S., Su, S., Kang, S. The oil shale formation mechanism of the Songliao Basin Nenjiang Formation triggered by marine transgression and oceanic anoxic events 3. *Oil Shale,* 2021, **38**(2), 89–118. https://doi.org/10.3176/oil.2021.2.01

8. Lin, F., Qi, L., Zhang, N., Guo, Z. An ongoing lithospheric dripping process beneath northeast China and its impact on intraplate volcanism. *Geology*, 2024, **52**(6), 435–440. https://doi.org/10.1130/g51861.1
9. Feng, Z., Jia, C. Z., Xie, X. N., Zhang, S., Feng, Z. H., Cross, T. A. Tectonostratigraphic units and stratigraphic sequences of the nonmarine Songliao Basin, northeast China. *Basin Res.*, 2010, **22**(1), 79–95. https://doi.org/10.1111/j.1365-2117.2009.00445.x
10. Zhang, J., Bian, X. F., Su, F. Research on the hydrocarbon generation potential of the Permian Linxi Formation in the Lu D1 well in the Zharut area of Inner Mongolia. *J. Pet. Nat. Gas.*, 2013, **35**, 63–67 (in Chinese with English abstract).
11. Su, F., Zhang, H. H., Zhang, J. Research on the hydrocarbon generation potential of the Permian Linxi Formation in the Tao D1 well in the Tao Haiyingzi area. *J. Yangtze Univ.*, 2016, **13**, 19–23 (in Chinese with English abstract).
12. Hu, X., Zhang, X., Xie, J., Cao, H., Zheng, X., Zhao, Z., Cao, J., Pu, Q., Li, Z., Zhou, L. Sedimentary characteristics and hydrocarbon-generation potential of the Permian Pingdiquan Formation in Dongdaohaizi Sag, Junggar Basin, northwest China. *ACS Omega*, 2023, **8**(39), 35653–35669. https://doi.org/10.1021/acsomega.3c01889
13. Sun, L., Chen, S. W., Zhang, J., Su, F., Bian, X. F., Zhang, H. H. Evaluation on the hydrocarbon generation potential of Upper Permian Linxi Formation in western slope of Songliao Basin: evidence from JBD-2 well. *Geol. Resour.*, 2021, **30**(3), 333–340 (in Chinese with English abstract).
14. Li, F., Zhang, C., Xue, H., Huang, W., Wang, K., Chen, Y., Zhou, Y. Evaluation of hydrocarbon generation potential of Laiyang Formation source rocks in Ri-Qing-Wei Basin, eastern Shandong. *Energies*, 2022, **15**(20), 7549. https://doi.org/10.3390/en15207549
15. Liang, C., Liu, Y., Zheng, C., Li, W., Neubauer, F., Zhang, Q. Macro- and microstructural, textural fabrics and deformation mechanism of calcite mylonites from Xar Moron-Changchun dextral shear zone, northeast China. *Acta Geol. Sin. Engl. Ed.*, 2019, **93**(5), 1477–1499. https://doi.org/10.1111/1755-6724.14357
16. Han, G., Liu, Y., Neubauer, F., Genser, J., Zou, Y., Li, W., Liang, C. Characteristics, timing, and offsets of the middle-southern segment of the western boundary strike-slip fault of the Songliao Basin in northeast China. *Sci. China: Earth Sci.*, 2012, **55**(3), 464–475. https://doi.org/10.1007/s11430-012-4362-y
17. Ren, J., Jin, J., Xiang, B., Ma, W., Zhou, N., Liao, J. Differences and genesis of shale oil properties between the upper and lower sections of the Lucaogou Formation in the Jimsar Sag. *IOP Conf. Ser.: Earth Environ. Sci.*, 2019, **360**(1), 012032. http://dx.doi.org/10.1088/1755-1315/360/1/012032
18. Du, J., Zhao, Y., Wang, Q., Yu, Y., Xiao, H., Xie, X., Du, Y., Su, Z. Geochemical characteristics and resource potential analysis of Chang 7 organic-rich black shale in the Ordos Basin. *Geol. Mag.*, 2018, **156**(7), 1131–1140. https://doi.org/10.1017/S0016756818000444
19. Shi, Y., Shi, S., Liu, Z., Liu, J., Ju, N., You, H., Zhang, Z., Zhao, C. Petrogenesis of the late Early Palaeozoic adakitic granitoids in the southern margin of the

Songliao Basin, NE China: implications for the subduction of the Palaeo-Asian Ocean. *Geol. J.*, 2018, **54**(6), 3821–3839. https://doi.org/10.1002/gj.3377
20. Chen, C., Ren, Y.-S., Zhao, H.-L., Zou, X.-T., Yang, Q., Hu, Z.-C. Permian age of the Wudaogou Group in eastern Yanbian: detrital zircon U–Pb constraints on the closure of the Palaeo-Asian Ocean in northeast China. *Int. Geol. Rev.*, 2014, **56**(14), 1754–1768. https://doi.org/10.1080/00206814.2014.956348
21. Ren, S. M., Qiao, D. W., Zhang, X. Z. Research progress on strategic selection areas of Upper Paleozoic oil and gas resources in the Songliao Basin and its periphery. *Geol. Bull.*, 2011, **101**, 197–204 (in Chinese with English abstract).
22. Zhong, M. S., Lu, D. L. Petrochemical characteristics and sedimentary structural environment of the Linxi Formation in the Suolun area of the middle section of the Greater Hinggan Range. *Geol. Surv. China*, 2022, **9**, 89–96 (in Chinese with English abstract).
23. Li, L., Hou, Q., Huang, D., Wang, X. Early Permian granitic magmatism in middle part of the northern margin of the North China Craton: petrogenesis, source, and tectonic setting. *Minerals*, 2021, **11**(2), 99. https://doi.org/10.3390/min11020099
24. Zhang, J., Xu, X., Bai, J., Chen, S., Liu, W., Li, Y. Accumulation and exploration of continental shale gas resources of Cretaceous Shahezi Formation in Lishu fault depression, Songliao Basin, NE China. *Pet. Explor. Dev.*, 2022, **49**(3), 502–515.
25. Hou, L., Huang, H., Yang, C., Ma, W. Experimental simulation of hydrocarbon expulsion in semi-open systems from variable organic richness source rocks. *ACS Omega*, 2021, **6**(22), 14664–14676. https://doi.org/10.1021/acsomega.1c01800
26. Xu, H., Xie, Q., Wang, S., Yu, S. Organic geochemical characteristics and gas prospectivity of Permian source rocks in western margin of Songliao Basin, northeastern China. *J. Pet. Sci. Eng.*, 2021, **205**(8), 108863. https://doi.org/10.1016/j.petrol.2021.108863
27. Wang, L., Zhang, Y., Xing, E., Peng, Y., Yu, D. Distribution of trace elements, Sr-C isotopes, and sedimentary characteristics as paleoenvironmental indicator of the Late Permian Linxi Formation in the Linxi Area, eastern Inner Mongolia. *J. Chem.*, 2020, **1**, 1–17.
28. Wang, X., Ren, Y.-S., Bo, J.-W., Zhao, D.-S. Provenance, tectonic setting and mineralization significance in the Linxi Formation, eastern Inner Mongolia, NE China. *Geochem.: Explor. Environ. Anal.*, 2019, **20**(1), 50–67.
29. Jansonius, J. *Palynology of Permian and Triassic Sediments, Peace River Area, Western Canada*. Nägele u. Obermiller, Stuttgart, 1962, 35–98.
30. Qu, T., Huang, Z., Li, T., Yang, Y., Wang, B., Wang, R. Sedimentology and geochemistry of Eocene source rocks in the East China Sea: controls on hydrocarbon generation and source rock preservation. *J. Asian Earth Sci.*, 2023, **255**, 105770. https://doi.org/10.1016/j.jseaes.2023.105770
31. He, X., Lu, J., Li, S., Li, X., Li, X., Chen, S., Li, Y., He, Q., Zhao, L., Ma, Z. Geochemical characteristics and hydrocarbon expulsion efficiency of different types of shale: taking Chang 7 Member and Shanxi Formation in Ordos Basin, China, as examples. *J. Energy Eng.*, 2023, **149**(5). https://doi.org/10.1061/JLEED9.EYENG-4854

32. Qu, Y., Tao, H., Ma, D., Wu, T., Qiu, J. Biomarker characteristics and geological significance of middle and upper Permian source rocks in the southeastern Junggar Basin. *Pet. Sci. Technol.*, 2019, **37**(19), 2066–2080. https://doi.org/10.1080/10916466.2019.1615950
33. Yang, Z., Li, Q., Qi, X., Yang, D. A new possible giant hydrocarbon generated formation: the Upper Triassic source rock in southwestern Junggar Basin, NW China. *Mar. Pet. Geol.*, 2017, **88**, 575–586. https://doi.org/10.1016/j.marpetgeo.2017.09.007
34. Feng, Z., Liu, D., Huang, S., Gong, D., Peng, W. Geochemical characteristics and genesis of natural gas in the Yan'an gas field, Ordos Basin, China. *Org. Geochem.*, 2016, **102**, 67–76. https://doi.org/10.1016/j.orggeochem.2016.10.008
35. García García, N., Feranec, R. S., Arsuaga, J. L., Bermúdez de Castro, J. M., Carbonell, E. Isotopic analysis of the ecology of herbivores and carnivores from the Middle Pleistocene deposits of the Sierra de Atapuerca, northern Spain. *J. Archaeol. Sci.*, 2009, **36**(5), 1142–1151. https://doi.org/10.1016/j.jas.2008.12.018
36. Wang, D., Mao, Q., Liu, K., Lyu, D., Liu, H., Yin, Y., Hu, H. Genetic mechanism of Carboniferous-Permian coal measures siderite nodules in an epicontinental sea basin – an example from the Zibo area in North China. *Ore Geol. Rev.*, 2023, **154**, 105254. https://doi.org/10.1016/j.oregeorev.2022.105254
37. Gao, G., Ren, J., Yang, S., Xiang, B., Zhang, W. Characteristics and origin of solid bitumen in glutenites: a case study from the Baikouquan Formation reservoirs of the Mahu Sag in the Junggar Basin, China. *Energy Fuels*, 2017, **31**(12), 13179–13189. https://doi.org/10.1021/acs.energyfuels.7b01912
38. Lu, J. C., Wei, X. Y., Wei, J. S. Characteristics and influencing factors of kerogen isotopes in Carboniferous-Permian source rocks in Ejina Banner and adjacent areas in western Inner Mongolia. *Geol. Bull.*, 20l0, **29**, 384–391 (in Chinese with English abstract).
39. Gong, F. H., Chen, S. W., Zhang, J. Study on the thermal evolution degree of Upper Permian Linxi Formation mudstone in Taohaiyingzi area, Inner Mongolia. *Geol. Resour.*, 2012, **21**, 129–133 (in Chinese with English abstract).
40. Xie, Z., Wei, G., Zhang, J., Yang, W., Zhang, L., Wang, Z., Zhao, J. Characteristics of source rocks of the Datangpo Fm, Nanhua System, at the southeastern margin of Sichuan Basin and their significance to oil and gas exploration. *Nat. Gas Ind. B*, 2017, **4**(6), 405–414. https://doi.org/10.1016/j.ngib.2017.09.011
41. Dean, R. A., Whitehead, E. V. The occurrence of phytane in petroleum. *Tetrahedron Lett.*, 1961, **2**(21), 768–770. https://doi.org/10.1016/S0040-4039(01)99264-0
42. Wang, C., Liu, Y., Liu, H., Zhu, L., Shi, Q. Geochemical significance of the relative enrichment of pristane and the negative excursion of δ13CPr across the Permian-Triassic Boundary at Meishan, China. *Chin. Sci. Bull.*, 2005, **50**(19), 2213–2225. https://doi.org/10.1007/BF03182673
43. Shanmugam, G. Significance of coniferous rain forests and related organic matter in generating commercial quantities of oil, Gippsland Basin, Australia. *AAPG Bull.*, 1985, **69**(8), 1241–1254. http://dx.doi.org/10.1306/AD462BC3-16F7-11D7-8645000102C1865D

44. Shen, Y., Qin, Y., Cui, M., Xie, G., Guo, Y., Qu, Z., Yang, T., Yang, L. Geochemical characteristics and sedimentary control of Pinghu Formation (Eocene) coal-bearing source rocks in Xihu Depression, East China Sea Basin. *Acta Geol. Sin. Engl. Ed.*, 2021, **95**(1), 91–104. https://doi.org/10.1111/1755-6724.14624
45. Qu, Y., Shan, X., Du, T., Du, X., Zhao, R. Molecular organic geochemical characteristics and coal gas potential evaluation of Mesozoic coal seams in the Western Great Khingan Mountains. *Acta Geol. Sin. Engl. Ed.*, 2020, **94**(2), 409–417. https://doi.org/10.1111/1755-6724.14297
46. Miao, H., Wang, Y., Zhao, S., Guo, J., Ni, X., Gong, X., Zhang, Y., Li, J. Geochemistry and organic petrology of Middle Permian source rocks in Taibei Sag, Turpan-Hami Basin, China: implication for organic matter enrichment. *ACS Omega*, 2021, **6**(47), 31578–31594. https://doi.org/10.1021/acsomega.1c04061
47. Nelson, C. R., Li, W., Lazar, I. M., Larson, K. H., Malik, A., Lee, M. L. Geochemical significance of *n*-alkane compositional-trait variations in coals. *Energy Fuels*, 1998, **12**(2), 277–283. https://doi.org/10.1021/ef970112k
48. Zheng, Y. J., Huang, X., Sun, Y. W. Division and correlation of carboniferous Permian system in Songliao Basin and its periphery. *Geo. Resour.*, 2018, **27**(1), 1–15 (in Chinese with English abstract).
49. Su, F., Bian, X. F., Wang, Q. H. Organic geochemical characteristics of source rocks of the Linxi Formation of Well Lu D2 in Zalut area, Inner Mongolia. *Geo. Bull*., 2013, **8**, 1307–1314 (in Chinese with English abstract).
50. Jarvie, D. M., Hill, R. J., Ruble, T. E., Pollastro, R. M. Unconventional shale-gas systems: the Mississippian Barnett Shale of north-central Texas as one model for thermogenic shale-gas assessment. *AAPG Bull*., 2007, **91**(4), 475–499. https://doi.org/10.1306/12190606068